Hindawi
Advances in Materials Science and Engineering
Volume 2022, Article ID 3658617, 6 pages
https://doi.org/10.1155/2022/3658617

Research Article

Axial Compressive Behavior of Lithium Slag Recycled Coarse Aggregate Concrete-Filled Circular Steel Stub Columns

Qiao-Huan Wang,[1,2] Jiong-Feng Liang,[3] Chun-Feng He,[3] and Wei Li[4]

[1]*School of Water and Environment, Chang'an University, Xi'an, China*
[2]*School of Water Resources and Environmental Engineering, East China University of Technology, Nanchang, China*
[3]*Faculty of Civil & Architecture Engineering, East China University of Technology, Nanchang, China*
[4]*College of Civil Engineering and Architecture, Wenzhou University, Wenzhou, Zhejiang, China*

Correspondence should be addressed to Wei Li; liw1981@126.com

Received 21 June 2021; Accepted 26 January 2022; Published 22 February 2022

Academic Editor: Robert Černý

In order to study the axial compression performance of lithium slag recycled concrete short columns in circular steel tubes, eight short columns were designed and tested. The main influence parameters of the specimens are lithium slag replacement rate and recycled concrete replacement rate. The test process and failure mode of the specimens are observed, and the load-displacement curve is drawn. The influence of the replacement rate on the axial compression performance of the specimens is analyzed. The results show that recycled concrete replacing natural coarse aggregate will reduce the mechanical properties of specimens, but lithium slag mixed into recycled concrete can compensate for the lack of mechanical properties of recycled concrete, and the specimens mixed with lithium slag and recycled concrete have good stiffness and ductility.

1. Introduction

The application of concrete-filled steel tubular structure in practical engineering can be traced back to the 1880s. The structure appeared in the form of piers in the British Severn Railway Bridge. With the development of concrete-filled steel tubular structure, the structure has been widely used in practical engineering in recent years and has shown diversified prospects in the development of construction industry. With the rapid development of urbanization, large amount of construction waste is produced. In order to solve the problem of construction waste stacking, realize the secondary utilization of resources, and protect the sustainable development of ecological environment, recycled coarse aggregate concrete emerges as the times require. Recycled concrete is a kind of coarse aggregate made from waste concrete after crushing and screening, which is used to replace natural coarse aggregate to realize the secondary utilization of construction dumping [1]. Since the 21st century, a large number of scholars have studied recycled concrete.

O'Mahony [2] studied the shear strength of recycled aggregate and compared the test results with those of natural aggregate. The results show that there seems to be no difference between the shear strength of limestone (standard natural aggregate) and that of recycled aggregate with friction angle of 54° and 58° at high density. The results of Arun et al. [3] show that the compressive strength, splitting tensile strength, and flexural strength of recycled coarse aggregate concrete are satisfactory, and the W/C ratio can be further reduced to improve the compressive strength of recycled coarse aggregate concrete. The test results of Tabsh and Abdelfatah [4] show that the loss rate of recycled concrete is higher than that of natural aggregate, but it is still acceptable. The compressive strength and splitting tensile strength of recycled coarse aggregate concrete depend on the mix proportion. In general, the strength of recycled concrete is 10–25% lower than that of traditional concrete made of natural coarse aggregate. The research of Tam et al. [5]shows that the failure mode of recycled concrete-filled steel tube is

similar to that of ordinary concrete-filled steel tube under axial compression.

Chen et al. [6] carried out a bending test on lithium slag concrete beams and a bending test on lithium slag concrete beams. The results show that adding lithium slag into concrete can increase the cracking load and ultimate load of beam, reduce the maximum crack width, and improve the corrosion resistance. He et al. [7] studied the effect of lithium slag on the mechanical properties of concrete. The results show that the compressive strength, elastic modulus, dry shrinkage, and creep of mature concrete can be improved by adding appropriate amount of lithium slag into concrete. To clarify the properties of LS powder as a supplementary cementitious material, Zhai et al. [8] studied the ionic solubility of LS powder and the hydration characteristics and hydration kinetics of LS powder mixed with cement.

Tan et al. [9] prepared nano-lithium slag by the wet grinding method and studied the effect of nano-lithium slag on the hydration mechanism of sulphoaluminate cement. The results indicated that nano-LS with D50 of 300 nm was prepared. In comparison with the previous studies, 4.0% nano-LS promoted the 7 h compressive strength from 4.5 MPa to 24.3 MPa, with an increase by more than 4 times and an increase by 28% at 1 d age; it also reduced the initial and final setting time to 16 min and 23 min, being reduced by 33.3% and 37.5%. He et al. [10] studied the effect of partial substitution of silica fume by lithium slag on the compressive strength and microstructure evolution of ultra-high-performance concrete. The results show that the use of lithium slag degrades the microstructure of ultra-high-performance concrete at early ages. However, the use of lithium slag with the appropriate content improves microstructure of ultra-high-performance concrete at later ages. The use of lithium slag improves the hydration degree of ultra-high-performance concrete and increases the elastic modulus of interfacial transition zone in ultra-high-performance concrete.

According to the research of many scholars, adding lithium slag into recycled concrete can make up for the lack of mechanical properties of recycled concrete.

Based on the above research conclusions, this paper puts forward the lithium slag recycled concrete structure of circular steel tube, carries out the axial compression test research on it, and analyzes the influence of lithium slag and recycled concrete replacement rate on the load-displacement relationship and bearing capacity of circular steel tube concrete column.

2. Experimental Programme

2.1. Specimen Design. Eight specimens are designed to study the axial compression performance of lithium slag recycled concrete short columns in circular steel tubes. All specimens have the same dimension with an external diameter of 89 mm, a thickness of 3 mm, and a length of 300 mm. The design parameters of tested specimens are shown in Table 1. Specifically, lithium slag (LS) replacement rate η refers to the quality rate of lithium slag in the sum of cement and lithium slag, which is 0%, 10%, 20%, and 30%, respectively. The recycled coarse aggregate (RCA) replacement rate r refers to the quality rate of RCA in all coarse aggregates, which is 0%, 30%, 50%, 70%, and 100%, respectively.

2.2. Material Properties. Commercial Portland cement with a 28-day nominal compressive strength of 42.5 MPa is used. The lithium slag (LS) with the appearance color of brown-black from Jiangxi lithium salt plant in China is used, which is shown in Figure 1. Table 2 lists the chemical composition of cement and LS. The recycled coarse aggregate (RCA) adopted in the test is produced from the waste concrete in Nanchang city, Jiangxi Province. The natural crushed stone and river sand are adopted as the natural coarse aggregates (NCA) and fine aggregates. Table 1 gives the mixture ratio of the new concrete. The average compressive strength f_{cu} of this concrete is also given in Table 1.

The welded circular hollow steel tube is used in this test. The yield strength and elastic modulus are 426 MPa and 203 GPa, respectively.

2.3. Experiment Setup. The tested columns are tested in a compression testing machine with a capacity of 3000 kN, which is shown in Figure 2. Each specimen is positioned on the supports to ensure its centerline is in line with the axis of the testing machine. The applied load is monitored by a 3000 kN capacity load cell. The axial deformation of the tested specimen is measured by the linear voltage displacement transducer (LVDT). The load and displacement data in the test are collected by the data acquisition instrument.

3. Results and Discussion

3.1. Failure Mode. Through the observation and analysis of the experimental process of the tested specimens, it is found that the failure modes of the specimens are basically similar, and there are certain rules: at the initial stage of loading, the specimens are in the elastic stage, and there is no obvious change on the surface. When the load reaches 80%~85% of the ultimate bearing capacity, the coating on the surface of the specimen peels off and the volume expands slightly; after reaching the ultimate bearing capacity, because the steel tube and core concrete have different elastic moduli, the deformation is different, resulting in different degrees of bulging phenomenon in the upper, middle, and lower parts of most specimens. Under the action of continuous load, the local bulging phenomenon of steel tube is intensified, and some specimens are cracked at the bulging place. The failure mode of lithium slag recycled coarse aggregate concrete-filled circular steel tube stub column is similar to that of ordinary concrete-filled circular steel tube stub column [11], and the final failure mode of the specimen is shown in Figure 3.

3.2. Load-Displacement Relationship. Figure 4(a) shows the load-displacement curves of the specimens with different LS replacement rates. It shows that the ultimate bearing

Table 1: Details of all specimens.

Specimen no.	r (%)	η (%)	RCA (kg·m^{-3})	LS (kg·m^{-3})	Crushed stone (kg·m^{-3})	Sand (kg·m^{-3})	Cement (kg·m^{-3}	Water (kg·m^{-3})	f_{cu} (MPa)
C1	0	0	0	0	1922	824	740	190	27.0
C2	0	10	0	74	1922	824	666	190	28.9
C3	0	20	0	148	1922	824	592	190	31.0
C4	0	30	0	222	1922	824	518	190	29.2
C5	30	20	577	148	1345	824	592	190	29.6
C6	50	20	961	148	961	824	592	190	28.2
C7	70	20	1345	148	577	824	592	190	26.8
C8	100	20	1922	148	0	824	592	190	25.9

Figure 1: Lithium slag.

Table 2: Chemical composition of cement and LS (%).

Material	SiO_2	Al_2O_3	Fe_2O_3	CaO	Na_2O	TiO_2	MgO	SO_3	K_2O	Loss
Cement	21.01	4.55	3.43	61.62	0.08	0.07	1.27	2.38	0.75	4.84
LS	45.90	19.30	1.23	9.70	0.31	2.20	1.10	5.97	1.20	13.09

Figure 2: Test setup.

(a) (b) (c)

Figure 3: Typical failure modes of tested specimens. (a) C1. (b) C4. (c) C6.

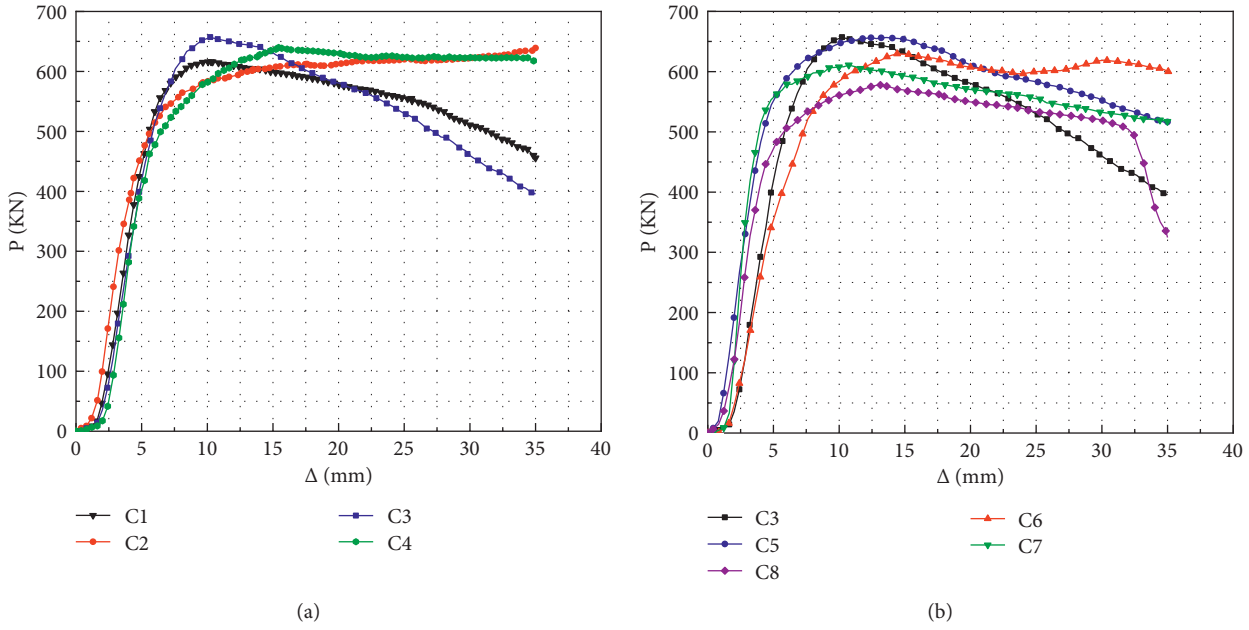

(a) (b)

Figure 4: Load-displacement curve of tested specimen. (a) Load-displacement curve with different LS replacement rates. (b) Load-displacement curve with different RCA replacement rates.

capacity of specimen C1 with lithium slag replacement rate of 0% is 616.04 kN. When the lithium slag replacement rates are 10%, 20%, and 30% respectively, the ultimate bearing capacity of the specimen increases by 4.3%, 6.9%, and 3.9%. With the substitution rate of lithium slag increasing from 0% to 30%, the linear slope of the elastic phase of the specimen has no obvious change because the lithium slag has no obvious effect on the stiffness of the specimen. After reaching the ultimate bearing capacity, the curves of specimens C1 and C3 decrease slightly, and the curves of specimen C2 still increase slowly after entering the plastic stage. Specimen C3 has no downward trend after reaching the ultimate bearing capacity, and the curves after the peak loading are very gentle.

Figure 4(b) shows the load-displacement curves of the specimens with different RCA replacement rates. With the RCA replacement rate increasing from 0 to 100%, the slope of the specimen in the elastic stage decreases slightly, and the longitudinal displacement increases relatively when it reaches the ultimate load, which is mainly because the stiffness of the specimen decreases with the increase of the RCA replacement rate. After reaching the ultimate bearing capacity, the load-displacement curve of each specimen decreases in varying degrees, and the decrease degree is slightly

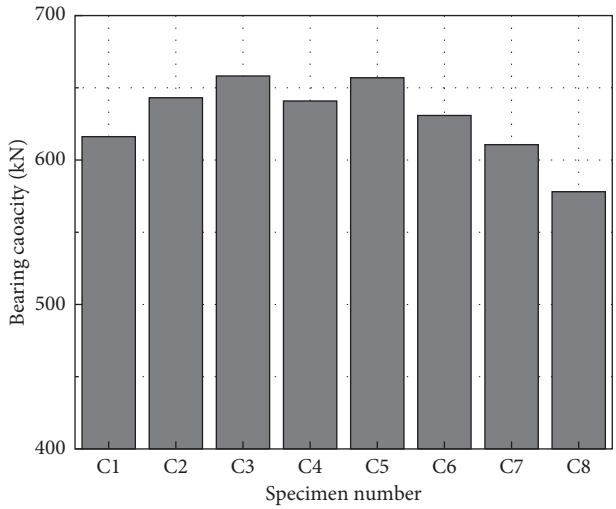

Figure 5: Comparison of bearing capacity of tested specimens.

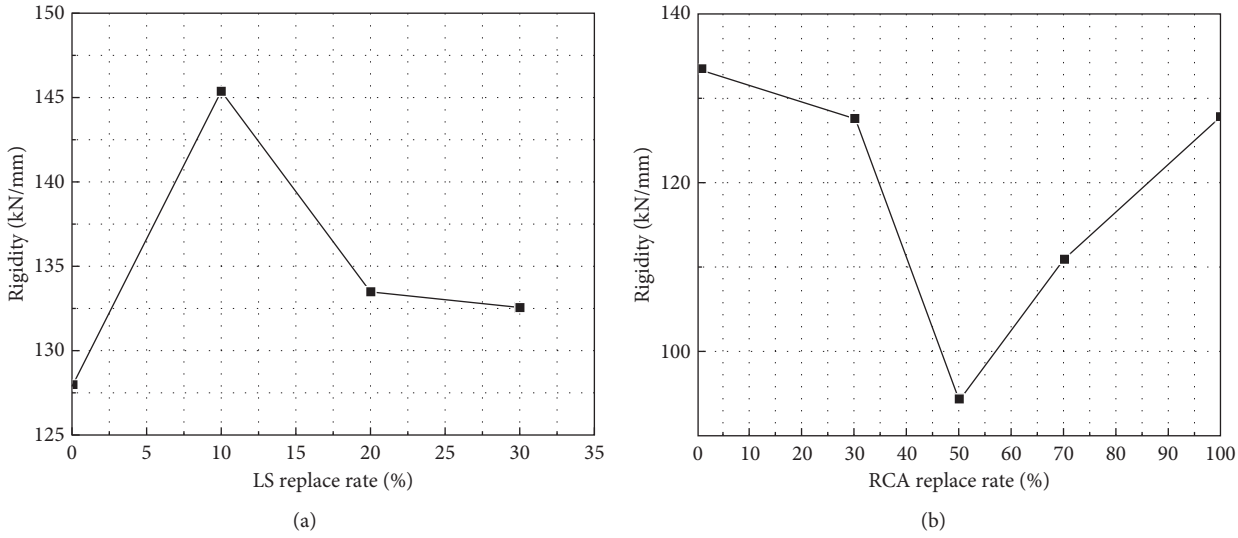

Figure 6: Effect of different parameters on the stiffness of specimens.

smaller than that of specimen C2 with 0% recycled concrete replacement rate. The load-displacement curve of specimen C8 has an obvious sudden drop stage, which is caused by the two cracks formed during the loading process, which are connected into one and finally extended to the top, and the specimen is completely destroyed. For the load-displacement curve of specimen C6 with 50% RCA replacement rate, the load begins to decline gently after reaching the ultimate bearing capacity, and the load rises slightly as the loading continues. This stage is the strengthening stage, and the ductility of the specimens is improved [12]. This phenomenon shows that the lithium slag and recycled concrete have good ductility and can continue to bear the load without being completely destroyed after the specimen is obviously deformed.

3.3. Bearing Capacity. Figure 5 shows the comparison of ultimate bearing capacity of tested specimens under axial compression loading. It can be seen from the figure that the ultimate load of the specimen is 616.04 kN, 643.04 kN, 658.50 kN, and 640.64 kN, respectively, when the substitution rate of LS is 0%, 10%, 20%, and 30%. With the increase of the substitution rate of lithium slag, the ultimate bearing capacity of the specimen first increases and then decreases. When the substitution rate of lithium slag is 20%, the ultimate bearing capacity of the specimen is the largest, which is 6.9% higher than that of the specimen with 0% substitution rate of lithium slag. When the replacement rate of lithium slag is 20%, the RCA replacement rate is changed. When the RCA replacement rate is 0%, 30%, 50%, 70%, and 100%, the ultimate bearing capacity of the specimen is

658.50 kN, 631.26 kN, 616.12 kN, 598.97 kN, and 588.75 kN, respectively. The replacement rate of recycled concrete increases from 0% to 100%, and the bearing capacity of specimens decreases by 13.2% [13].

3.4. Stiffness. Figure 6 shows the effect of LS replacement rate and RCA replacement rate on the stiffness of the specimens. It can be seen from Figure 6(a) that the incorporation of lithium slag can improve the elastic modulus of core concrete and then improve the stiffness of the specimen, up to 13.8%. It can be seen from Figure 6(b) that the stiffness of the specimen decreases with the addition of RCA. The main reason may be that the elastic modulus of the core concrete decreases with the addition of recycled coarse aggregate, which further reduces the axial compression stiffness of the specimen.

4. Conclusions

Based on the above research results, the following conclusions can be drawn:

(i) The failure mode of all specimens is strength failure, and the process of slight expansion, bulging deformation, and overall failure occurs in turn. The bulging failure is probably distributed at the top, middle, and bottom, and the degree of bulging is different under different LS or RCA replacement rates, which is similar to the failure mode of ordinary concrete-filled circular steel tube stub column.

(ii) The substitution rate of LS and RCA has a certain influence on the ultimate bearing capacity of the specimens. With the increase of LS replacement rate, the ultimate load first increases and then decreases. With the increase of RCA, the ultimate load gradually decreases. In this test, the best replacement rate of lithium slag is 20%, and the replacement rate of recycled concrete is 30%~50%.

(iii) According to the observation and analysis of the whole process of the test, all the specimens have good stiffness and ductility. It can be concluded that the lithium slag recycled coarse aggregate concrete-filled circular steel stub columns have good deformation ability.

Data Availability

The data used to support the findings of this study are included within the article.

Conflicts of Interest

The authors declare that they have no conflicts of interest regarding the publication of this paper.

Acknowledgments

This study was supported by the Chinese National Natural Science Foundation (nos. 51868001 and 52068001), the Project of Academic and Technological Leaders of Major Disciplines in Jiangxi Province (no. 20204BCJL2037), and the Natural Science Foundation of Jiangxi Province (no. 20202ACBL214017).

References

[1] D. Katerusha, "Attitude towards sustainability, study contents and the use of recycled concrete in building construction-case study Germany and Switzerland," *Journal of Cleaner Production*, vol. 289, 2021.

[2] M. M. O'Mahony, "An analysis of the shear strength of recycled aggregates," *Materials and Structures*, vol. 30, no. 10, pp. 599–606, 1997.

[3] A. Arun, D. Chekravarty, and K. Murali, "Comparative analysis on natural and recycled coarse aggregate concrete," *Materials Today Proceedings*, 2021.

[4] S. W. Tabsh and A. S. Abdelfatah, "Influence of recycled concrete aggregates on strength properties of concrete," *Construction and Building Materials*, vol. 23, no. 2, pp. 1163–1167, 2009.

[5] V. Tam, Z. B. Wang, and T. Zhong, "Behaviour of recycled aggregate concrete filled stainless steel stub columns," *Materials and Structures*, vol. 47, pp. 293–310, 2014.

[6] L. Chen, J. Yao, and G. Zhang, "Flexural properties of lithium slag concrete beams subjected to loading and thermal-cold cycles," *KSCE Journal of Civil Engineering*, vol. 23, no. 3, 2018.

[7] Z. H. He, L. Y. Li, and S. G. Du, "Mechanical properties, drying shrinkage, and creep of concrete containing lithium slag," *Construction and Building Materials*, vol. 147, pp. 296–304, 2017.

[8] M. Zhai, J. Zhao, D. Wang, Y. Wang, and Q. Wang, "Hydration properties and kinetic characteristics of blended cement containing lithium slag powder," *Journal of Building Engineering*, vol. 39, Article ID 102287, 2021.

[9] H. Tan, M. Li, X. He, Y. Su, J. Yang, and H. Zhao, "Effect of wet grinded lithium slag on compressive strength and hydration of sulphoaluminate cement system," *Construction and Building Materials*, vol. 267, Article ID 120465, 2021.

[10] Z. H. He, S. Du, and D. Chen, "Microstructure of ultra high performance concrete containing lithium slag," *Journal of Hazardous Materials*, vol. 353, pp. 35–43, 2018.

[11] J. Chen, Y. Wang, C. W. Roeder, and J. Ma, "Behavior of normal-strength recycled aggregate concrete filled steel tubes under combined loading," *Engineering Structures*, vol. 130, pp. 23–40, 2017.

[12] M. X. Xiong, Z. Xu, G. Chen, and Z. H. Lan, "FRP-confined steel-reinforced recycled aggregate concrete columns: concept and behaviour under axial compression," *Composite Structures*, vol. 246, Article ID 112408, 2020.

[13] F. X. Ding, D. R. Lu, Y. Bai et al., "Behaviour of CFRP-confined concrete-filled circular steel tube stub columns under axial loading," *Thin-Walled Structures*, vol. 125, 2018.